

Effect of self heating on the torque vs. equivalent tensile strain plot in high temperature torsion of visco-plastic material

R. KOUITAT NJIWA

Laboratoire de Science et Génie des Surfaces UMR CNRS 7570, INPL-École des Mines; Université Henri Poincaré Nancy 1

G. MÉTAUER, A. MARCHAL*, J. VON STEBUT

Laboratoire de Science et Génie des Surfaces UMR CNRS 7570, INPL-École des Mines

In hot forming as simulated by the torsion test, a temperature rise due to self heating is simulated within a FEM approach. The numerical results allow for a “natural” explanation of the maximum experimentally observed for the torque vs. equivalent tensile strain plot. There is no longer any need for assumptions of microstructurally conditioned strain softening during the test. With increasing cumulated strain (time) the radial temperature gradient in a cross section of the useful centre part of the test specimen is shown to change in sign; in the beginning the temperature is highest at the surface and at the end the temperature maximum is at the centre. © 2001 Kluwer Academic Publishers

1. Introduction

A coherent model of the thermo-mechanical behaviour of materials is a basic requirement for realistic simulation of industrial hot forming operations.

The establishment of such a model generally requires the definition of various constitutive functions relating system variables like stress, strain and strain rate. In practice one postulates an *a priori* constitutive law depending on the material parameters. The results of bench marking experiments then allow for identification of these material specific parameters.

This is done for the torsion test, a well established method of studying solids heavily strained at high temperature. In particular, this test allows laboratory simulation under conditions of stress, strain and strain rate close to industrial practise. Torque (Γ), number of revolutions (N) and the instantaneous rotational speed (dN/dt) are the characteristic experimentally accessible parameters of this mechanical test (where only one end of the generally cylindrical specimen is rotated while the second one is maintained in a fixed grip).

In order to arrive at the constitutive laws one proceeds the following way: according to an approach due to Fields and Backofen, further developed by Rossard [1] the equivalent stress (σ_{eq}) at the surface of the specimen is determined. The parameters of the constitutive law are identified by means of the experimental equivalent stress σ_{eq} .

At high strain rates and high operation temperatures the Γ vs. N “torsion plots” of various steels have a local maximum (Fig. 1). Most frequently the decrease in measured torque is attributed to strain softening of the material. Indeed, when assuming isothermal test

conditions, the decrease in Γ implies a drop of σ_{eq} , suggesting a rearrangement of the material microstructure. As a logical consequence the constitutive law then becomes complicated in order to account for these structural modifications in the course of strain history.

Various of our torsion tests have evidenced a considerable self heating effect at the specimen surface. Therefore we have decided to evaluate thermal effects on the experimentally determined torsion plot. The approach chosen is numerical modelling of hot torsion of a visco plastic material. We then describe the material behaviour by a Norton-Hoff-type law without explicitly accounting for strain softening due to microstructure modifications. This is done intentionally in order to specifically reveal the effect of self heating on the shape of the torsion plot.

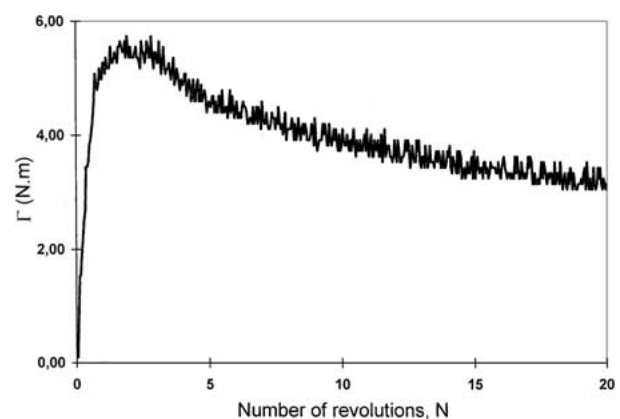


Figure 1 Example of an experimental hot torsion curve: torque vs. number of revolutions.

* Present Address: Peugeot SA.

2. System equations and numerical modelling

The cylindrical test specimen is supposed to be continuous, homogeneous, and isotropic. The deformation process is assumed to be governed by general thermo-mechanical equations

2.1. Momentum conservation

$$\text{Div} \Sigma + \vec{f} = \rho \vec{a} \quad (1)$$

With \vec{a} being the acceleration vector, \vec{f} the density of volume forces, ρ the mass density and Σ the Cauchy tensor. In the following the influence of \vec{a} and \vec{f} are neglected.

2.2. Energy conservation and equation of thermal transfer

The energy conservation law is formulated in the usual way

$$\rho \frac{D}{Dt} e = \Sigma : D + r - \text{Div} \vec{q}$$

This is a relation between the material derivative of the specific internal energy (e), the density of internal energy generated at a distance (r) the heat flow vector (\vec{q}), which represents the thermal conduction exchange and the stress power $\Sigma : D(\vec{u})$:

$D(\vec{u})$ is the of strain rate tensor associated to the velocity field \vec{u} .

Considering that the material under investigation is isotropic, the Fourier law leads to $\vec{q} = -\lambda \text{Grad}(T)$ where λ is the thermal conductivity of the material and T the absolute temperature. If we assume de-coupled thermal and mechanical energy dissipation the equation of heat transfer of our rigid visco-plastic specimen reads

$$\rho C_p \frac{D}{Dt} T = -\text{Div}(\lambda \text{Grad}(T)) - Q \quad (2)$$

Even though the specific heat C_p is strictly speaking a function of temperature, we assume it to be constant in our applications. Q is the amount of mechanical power dissipated per unit volume.

We can write explicitly $Q = \Sigma : D(\vec{u}) - A \cdot \dot{\alpha}$ where $\dot{\alpha}$ is the material derivative of an internal scalar variable related to the strain history and A is the corresponding thermodynamic driving force. The expression $A \cdot \dot{\alpha}$ is a

measure of the energy absorbed in microstructure material transformation. Most authors assume this energy to represent only a small fraction (roughly 10%) of the internal power dissipation. This leads to $Q = f \Sigma : D(\vec{u})$ where the coefficient f obeys $0.9 < f < 1$. In our application we will assume that all of the mechanical energy is dissipated as heat.

2.3. Constitutive material law

For hot forming operations one commonly supposes the material to behave essentially like a fluid (rigid viscoplastic model). The response of the material is often described by a law relating the Cauchy stress deviator to the strain rate. We shall adopt one of the most frequently applied models of the classical Norton-Hoff type.

$$S = 2K (\sqrt{3} \dot{\epsilon}_{eq})^{m-1} D(\vec{u}) \quad (3)$$

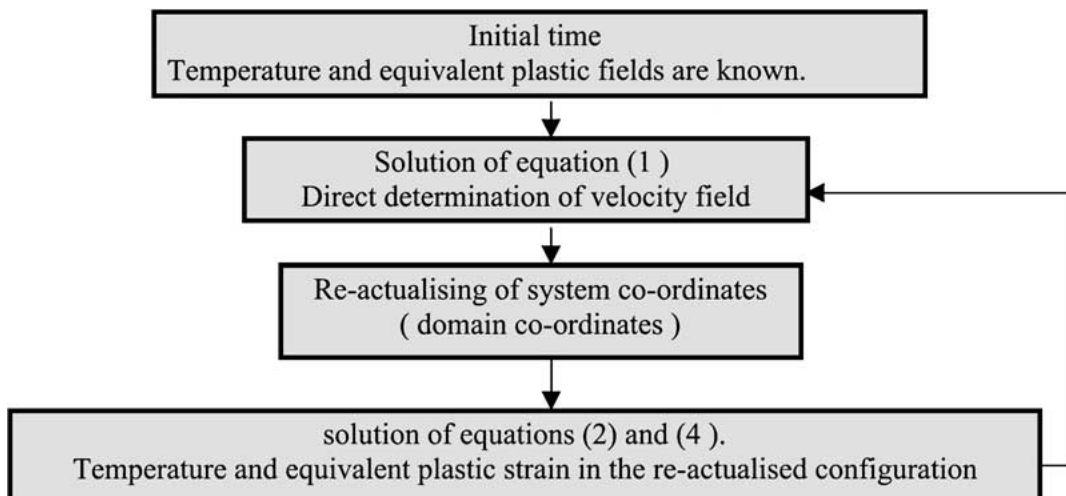
With $\dot{\epsilon}_{eq} = \sqrt{\frac{2}{3} D(\vec{u}) : D(\vec{u})}$ being the equivalent tensile strain rate (generalised strain rate). The material specific parameter m represents the strain rate sensitivity of stress. The parameter K is related to the consistency of the material. It depends on temperature and equivalent plastic tensile strain ($\bar{\epsilon}_{eq}$). We postulate $K = K_0 \exp(\beta/T) \bar{\epsilon}_{eq}^n$ where K_0 is a material constant, β the ratio of thermal activation energy (Q) by the Boltzmann constant (R). In order to account for the relation between K and $\bar{\epsilon}_{eq}$ the system equation is completed by the expression

$$\frac{D\bar{\epsilon}_{eq}}{Dt} = \dot{\epsilon}_{eq} \quad (4)$$

2.4. Solution strategy

With such a definition of the thermo-mechanical situation, the boundary conditions of Equations 1 and 2 have to be specified. In addition, it is generally admitted that plastic flow is incompressible. The velocity field which follows when solving Equation 1 must satisfy the constraint: $\text{tr}(D(\vec{u})) = 0$ ($\text{div} \vec{u} = 0$).

For the numerical treatment of the problem we adopt the strategy proposed by Zienkiewicz [2]. Its implementation is fairly simple. This method has already been applied successfully to forming operations by several authors (e.g. Kobayashi [3], Cormeau *et al.* [4]). It can be described by the following flowchart:



Within the context of this solution strategy the equations have to be re-written in a way suited for numerical approximation by the finite element method. We must consider the weak form of the problem already practised by various authors (cf. Zienkiewicz [2], Glowinski [5], Fortin and Glowinski [6]).

3. Results

The following analysis deals with cylindrical specimens of circular cross section and constant length. The axial symmetry allows for adoption of a two dimensional approach with cylindrical co-ordinates. The boundary conditions of Equation 2 specified in Fig. 2 all have the following form:

$$\lambda \text{Grad}(T) \cdot \vec{n} = -h(T)(T - T_a)$$

On the lateral surface this corresponds to heat exchange with the environment via radiation and/or convection. The transfer function is $h(T) = (h_a + \sigma_r \varepsilon_r (T + T_a)(T^2 + T_a^2))$ where h_a , σ_r , and ε_r (considered to be constants) are respectively the coefficients of convective exchange, the Stephan Boltzmann constant and the emissivity of the surface. The temperature of the environment, T_a , is also considered to be maintained constant during the test.

Heat exchange at the grips by conduction is considered to be described by a flat contact with a constant coefficient $h(T) = h_c$. It is well understood that this approach is an approximation only. Strictly speaking all of these “exchange coefficients” depend on temperature, specimen surface topography and nature.

3.1. Validation of the simulation code

The solution strategy described above has allowed decoupling of the thermal and mechanical aspects of the problem. The validation of the simulation code will be done by comparing the numerical and analytical solutions of the extreme situations; purely mechanical and purely thermal problems.

3.1.1. The purely mechanical situation

The purely mechanical situation corresponds to conventional isothermal test conditions of a cylindrical specimen with circular cross-section. It is sufficient to consider the useful centre part of the specimen only. The torque is computed by Zienkiewicz’s strategy of nodal stress extrapolation [7]. The analytically computed torque is described by the expression $\Gamma = \frac{2\pi}{3+m+n} K_0(\sqrt{3})^m \exp(\beta/T) \bar{\varepsilon}_R^n \dot{\varepsilon}_R^m R^{(3+m+n)}$ where R is the radius of the cylindrical test specimen, $\bar{\varepsilon}_R$ the equivalent plastic strain and $\dot{\varepsilon}_R$ the equivalent plastic strain rate at the surface of the useful centre part of the specimen.

The numerical and the analytical results for the torsion plot, Γ vs. N , are indistinguishable.

3.1.2. The purely thermal situation

In order to validate the purely thermal aspect of the code the analytical and numerical solutions have been compared for the following model situation of the temperature gradient along the radius of an infinite cylinder immersed from the very start into a heat bath of constant temperature T_a . Thus all of the cross sections along the specimen are equivalent. We suppose the heat exchange across the surface to be governed by convection only. For the numerical simulation we suppose no heat exchange via the the cross sections corresponding to the ends of the useful centre part. As to the analytical solution, it can be easily obtained by a finite Hankel transform [8]

$$T(r, t) = T_a + \frac{2(T_i - T_a)}{R} \sum_i \frac{\xi_i e^{-\chi \xi_i^2 t} J_0(\xi_i r) J_1(\xi_i R)}{(h^2 + \xi_i^2) [J_0(\xi_i R)]^2}$$

The sum is over all the positive roots of the transcendental equation $h J_0(\xi R) = \xi J_1(\xi R)$.

We define $h = h_c/\lambda$ and $\chi = \frac{\lambda}{\rho C_p}$. J_0 and J_1 are respectively the zero and first order Bessel functions of the first kind. T_i is the initial surface temperature of the test specimen. Here again excellent agreement has been achieved between the analytical and numerical solutions.

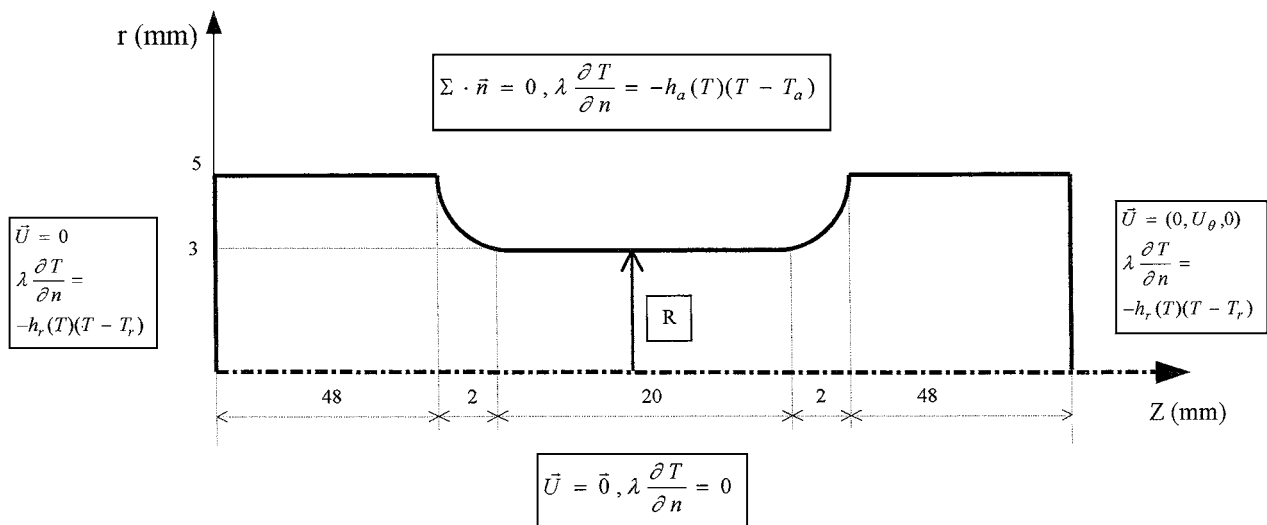


Figure 2 Torsion test specimen: boundary conditions of Equations 1 and 2.

$$\dot{N}(t) = \begin{cases} \left(2 \frac{t}{t_s} - \frac{t^2}{t_s^2}\right) N_0 & t \leq t_s \\ N_0 & t \geq t_s \end{cases}$$

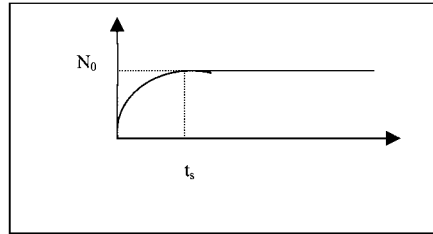


Figure 3 Start up rotation of the specimen.

3.2. Analysis of thermo-viscoplastic torsion

We are essentially interested in the influence of the thermal effect for specific steels on the Γ vs. N plot at high temperature. The results correspond to test conditions with equivalent strain rates of 10 s^{-1} . The results are presented as a function of the number of revolutions for the effective torque Γ (Fig. 6) as well as the absolute temperature T along the cylinder radius R (Fig. 7) of a cross section in the useful centre part.

The numerical results plotted out in the figures all correspond to the following values (in ISO units) assumed for the system constants.

$$\begin{aligned} K_0 &= 1.06 \cdot 10^{+6}; & \beta &= 6000; & n &= 0; & m &= 0.5; \\ \rho &= 7.8 \cdot 10^{+3}; & C_p &= 750; & &= 26; \\ h_a &= 20 \cdot 10^{+3}; & h_c &= 12 \cdot 10^{+3} \end{aligned}$$

In practise the nominal rotational speed is only attained with a small delay after the start of the experiment. This situation is schematically shown in Fig. 3. In our case the rise time t_s is always considered to be 0.3 s, corresponding to the execution of as much as 3.5 torsion cycles.

Let us first consider the case of specimens as defined in Fig. 1. We assume that inductive heating initially produces a uniform temperature distribution in the useful centre part of the specimen. The extremities of the specimens can either be assumed to have the same temperature as the centre part or to be close to room temperature as verified in our experiments.

When considering the system as thermally insulated (closed system) the results of our numerical simulations yield relative variations of temperature, equivalent stress and torque which are indistinguishable in the useful centre part of the specimen.

Fig. 4 shows these numerical results during a typical torsion test for the local temperature at 4 reference points (R/4, R/2, 3R/4, R), along the radius of cross section in the useful centre part. After 20 cycles the surface temperature rise is roughly 200°C . As expected, the higher the local strain rate the more important is the corresponding temperature rise. These numerical simulation results prove that the torsion test cannot be considered as isothermal and raise the question concerning the validity of the “zero radial temperature gradient” assumption retained within the Fields and Backoffen approach.

Owing to the variation of temperature during the torsion test the equivalent stress shows a clear maximum (Fig. 5). The position of this maximum shifts in time (to higher cycle numbers) as we approach the axis of

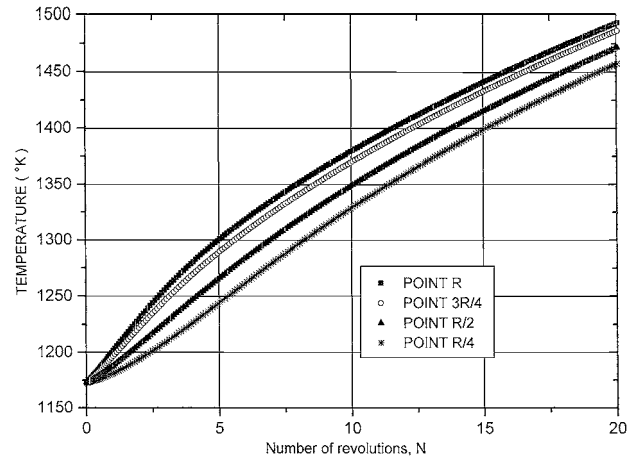


Figure 4 Temperature vs. number of revolutions at 4 reference points for an insulated system.

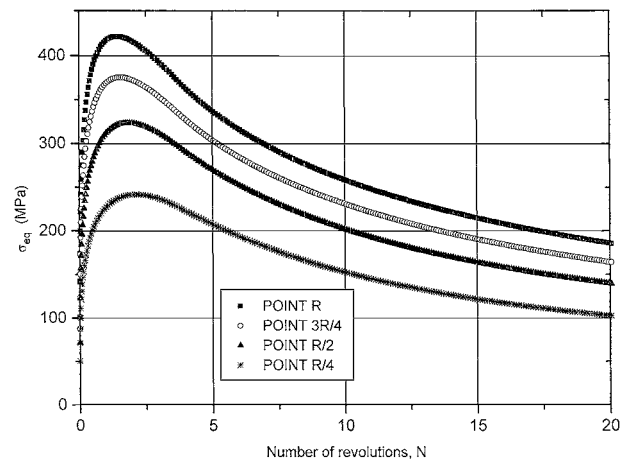


Figure 5 Equivalent plastic tensile stress vs. number of revolutions at 4 reference points for an insulated system.

symmetry of the specimen ($R \rightarrow R/4$). When comparing with Fig. 3 it is also evident that the maximum in equivalent stress, σ_{eq} , is attained already during the rise time before stabilisation of the rotational speed. The Γ vs. N plot (Fig. 6) also shows a maximum which is perfectly related to that of σ_{eq} and situated at the same position in time computed for “point R”. This is certainly due to the particular choice of our system parameters as the maximum of σ_{eq} is expected to be slightly delayed compared to that at the surface.

Owing to the absence of a thermal gradient along the specimen axis, the simulation can be simplified. Thus, if thermal exchange across the surface is taken into account, it is sufficient to only study the useful centre part of the specimen. Fig. 7 shows the corresponding temperature evolution across a cross section of the useful centre part. When comparing with the preceding

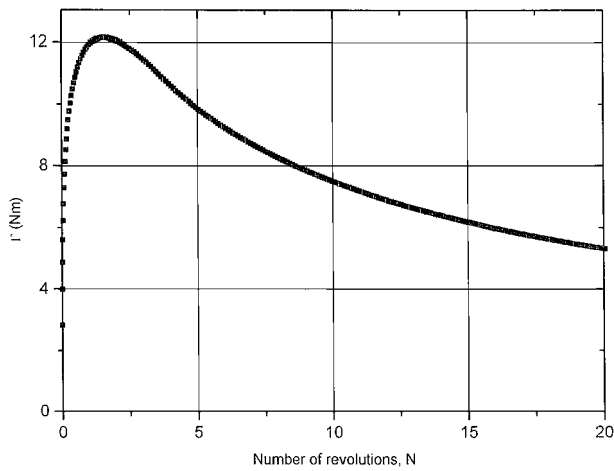


Figure 6 Torque vs. number of revolutions for an insulated system.

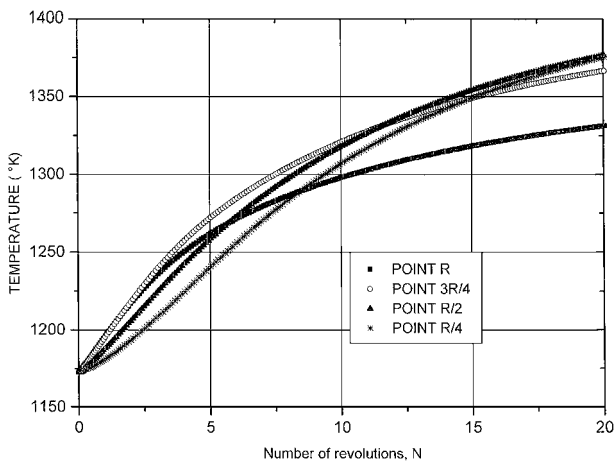


Figure 7 Temperature vs. number of revolutions at 4 reference points when lateral heat exchange is taken into account (the equivalent tensile strain rate is 10 s^{-1}).

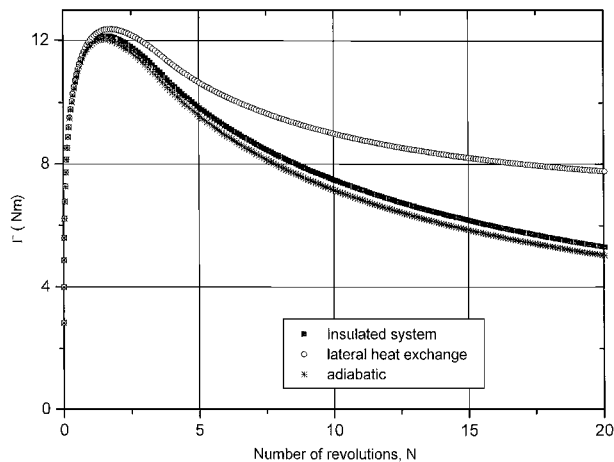


Figure 8 Torque vs. number of revolutions (insulated system, adiabatic system, lateral heat exchange).

situations (cf.: Fig. 4) the temperature “profile” is entirely modified. In the course of the test the hottest point progressively shifts from the surface to the centre of the test specimen. As is evident in Fig. 8, this modification of the radial temperature gradient also strongly influences the evolution of the effective torque during the torsion experiment. Notice that the maximum in torque is attained later than in the case of a closed system which approaches the behaviour for an adiabatic system.

4. Conclusion

We have presented a numerical FEM approach for hot forming as experimentally simulated by the torsion test of cylindrical specimens.

This has been done by taking into account energy dissipation via thermal effects and assuming rigid viscoplastic material behaviour.

Perfect agreement is obtained when validating the numerical model by comparing it to analytical results in the extreme case of purely mechanical and purely thermal mechanisms. The model is thus considered as validated in the mixed situation of joint thermal and mechanical situations.

We show that the experimentally well established maximum in the first part of the torque vs. equivalent tensile plastic strain plot can then be readily accounted for, without any sophisticated strain softening mechanisms due to microstructural modifications.

The torque maximum can be explained by self-heating of the specimen which continuously increases as the test continues. Thus the observed softening is mainly due to self-heating.

The specimen temperature at a characteristic cross section in the “useful” centre part of the specimen shows a clear gradient. In the beginning of the test the surface temperature is highest. As the experiment carries on (20 turns at a nominal equivalent tensile strain rate of 10 s^{-1}) this temperature gradient is inverted proving the influence of heat exchange with surrounding medium.

In conclusion, the general assumptions of isothermal experimental conditions, strain softening and zero temperature gradient along the radius of a representative specimen cross section appear to be unjustified.

Acknowledgements

This study has been done in association with the thesis work of A. Marchal whose experimental approach was backed-up by Peugeot SA. The authors acknowledge the considerable amount of work by C. Davoine who has built the torsion machine and has done all of the torsion experiments.

References

1. C. ROSSARD, in “Mise en forme des métaux et alliages” (CNRS, 1975) p. 39.
2. O. C. ZIENKIEWICZ, in “Numerical Analysis of Forming Processes” (J. Wiley & Sons, 1984) p. 1.
3. S. KOBAYASHI, in “Numerical Analysis of Forming Processes” (J. Wiley & Sons, 1984) p. 45.
4. A. CORMEAU, I. CORMEAU and J. ROOSE, in “Numerical Analysis of Forming Processes” (J. Wiley & Sons, 1984) p. 219.
5. R. GLOWINSKI, “Numerical Methods for non linear Variational Problems” (Springer-Verlag, 1982).
6. M. FORTIN and R. GLOWINSKI, “Méthodes de Lagrangien Augmenté: Application à la Résolution Numérique de Problèmes aux Limites” (Dunod, 1982).
7. O. C. ZIENKIEWICZ and J. Z. ZHU, *Int. J. Num. Meth. Eng.* **33** (1992).
8. I. SNEDDON, “Fourier Transform” (McGraw-Hill, 1951).

Received 21 July 2000
and accepted 9 July 2001